

Analyst

Accepted Manuscript

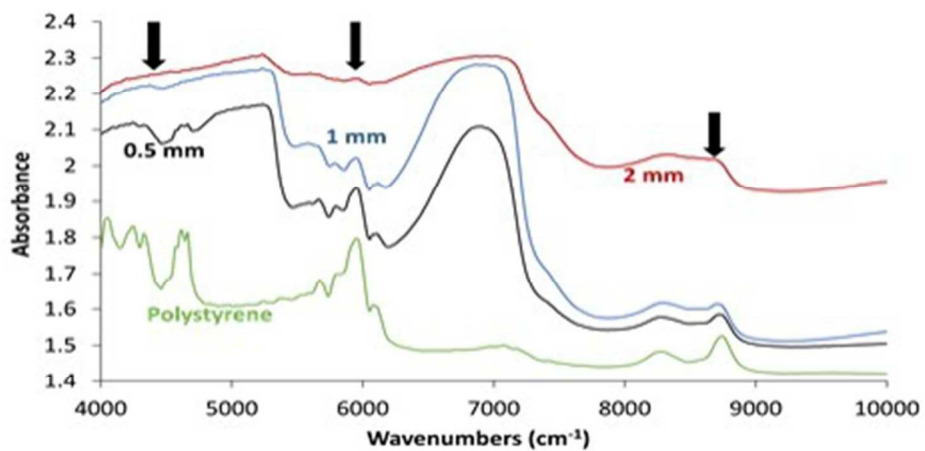


This is an *Accepted Manuscript*, which has been through the Royal Society of Chemistry peer review process and has been accepted for publication.

Accepted Manuscripts are published online shortly after acceptance, before technical editing, formatting and proof reading. Using this free service, authors can make their results available to the community, in citable form, before we publish the edited article. We will replace this *Accepted Manuscript* with the edited and formatted *Advance Article* as soon as it is available.

You can find more information about *Accepted Manuscripts* in the [Information for Authors](#).

Please note that technical editing may introduce minor changes to the text and/or graphics, which may alter content. The journal's standard [Terms & Conditions](#) and the [Ethical guidelines](#) still apply. In no event shall the Royal Society of Chemistry be held responsible for any errors or omissions in this *Accepted Manuscript* or any consequences arising from the use of any information it contains.



In this study we established how the depth of penetration into cartilage varies throughout the NIR frequency range (4000-10000 cm⁻¹).
79x40mm (150 x 150 DPI)

Wavelength-Dependent Penetration Depth of Near Infrared Radiation into Cartilage

M.V. Padalkar,^a and N. Pleshko^a

^a Department of Bioengineering, Temple University, Philadelphia, PA

Corresponding Author: Dr. Nancy Pleshko

Email: npleshko@temple.edu

Abstract

Articular cartilage is a hyaline cartilage that lines the subchondral bone in a diarthrodial joint. Near infrared (NIR) spectroscopy has been emerging as a nondestructive modality for evaluation of cartilage pathology. However, studies of the depth of penetration of NIR radiation into cartilage are lacking. The average thickness of human cartilage is about 1-3 mm, and it becomes even thinner as OA progresses. To ensure that the spectral data collected is restricted to the tissue of interest i.e. cartilage in this case, and not from the underlying subchondral bone, it is necessary to determine the depth of penetration of NIR radiation in different wavelength (frequency) regions. In the current study we establish how the depth of penetration varies throughout the NIR frequency range (4000-10000 cm⁻¹). NIR spectra were collected from cartilage samples of different thicknesses (0.5 mm to 5 mm) with and without polystyrene placed underneath. A separate NIR spectrum of polystyrene was collected as a reference. It was found that the depth of penetration varied from ~1 mm to 2 mm in the 4000-5100 cm⁻¹ range, to ~3 mm in the 5100-7000 cm⁻¹ range, and to ~5 mm in the 7000-9000 cm⁻¹ frequency range. These findings suggest that the best NIR region to evaluate cartilage only with no subchondral bone contribution is between 4000-7000 cm⁻¹.

Introduction

Articular cartilage is a hyaline cartilage that lines the subchondral bone in a diarthrodial joint. It is composed primarily of collagen type II, proteoglycans, cells and water. Cartilage has zonal organization with respect to depth, and is typically divided into a superficial, middle, deep and calcified zone. The cell morphology, collagen fiber orientation and composition varies throughout the zones¹. Water and collagen content vary from being greatest at the surface to lowest in deep zone. However, proteoglycan content has the opposite trend, with a lower content at the surface and higher content in the deep zone. The primary function of cartilage is to provide frictionless motion and act as a shock absorber. The mechanical properties of cartilage are due to its composition where collagen provides tensile strength and proteoglycans are responsible for compressive stiffness. The primary functions of water in cartilage are shock absorption during loading, transport of nutrients, and lubrication².

Osteoarthritis (OA) is a progressively disabling disease characterized by wear and tear of cartilage. Approximately 27 million adults in United States are estimated to have OA, with prevalence correlated with age and obesity³. The pathology of OA is characterized by a damaged collagen network, loss of proteoglycan, and an increase in water content, often resulting in fibrillation and thinning of articular cartilage⁴. Articular cartilage is avascular and acellular therefore it has very little capability to repair itself⁵. Clinically, arthroscopy has been used as a 'Gold Standard' to diagnose and treat intra-articular tissues, such as cartilage⁶, meniscus⁷, and ligament⁸ injuries. During standard arthroscopy procedures, the knee joint is filled with pressurized saline to keep the joint open as well as wash off the synovial fluid to give surgeons a clear view of cartilage. Surgeons can view the cartilage with the arthroscope on a monitor and make a decision on the quality of the cartilage. However, arthroscopic evaluations can be observer dependent^{9, 10}. More quantitative outcome measures are under development¹¹, including advanced magnetic resonance imaging (MRI) analyses. MRI has a long, though not entirely successful, record in the noninvasive evaluation of cartilage¹²⁻¹⁴. Limitations of the MRI approach include limited spatial resolution, lack of molecular specificity, and the difficulties of partial volume averaging effects. Thus, the detection of thin fissures, cartilage flaps, and shallow defects can present a substantial challenge^{15, 16}. Further, MRI is not typically utilized intra-operatively.

Fourier transform infrared (FT-IR) exhibits a high degree of specificity to molecular structure and compositional changes in tissue. The mid infrared (MIR) spectral absorbances from connective tissues are well understood, but MIR radiation exhibits a penetration depth of only ~10 microns through tissue, restricting its utility to the study of surface characteristics and degradation^{17, 18}. Near infrared (NIR) spectroscopy has been emerging as a nondestructive modality for cartilage evaluation¹⁹⁻²¹. It has been shown that NIR spectra correlate with cartilage matrix composition²²⁻²⁴,

1
2
3 thickness²⁵, mechanical response of intact and artificially degraded cartilage²⁶, degradation enzymatically²⁷, traumatic
4 degradation²⁸, as well as histological grading schemes, such as the Mankin score^{29, 30}. In addition, several studies are
5 advocating the use of NIR probes arthroscopically to evaluate early degeneration^{19, 21}. It is a well-known fact that NIR
6 penetrates to a much greater depth, ~mm to ~cm^{31, 32}. Several studies have shown that the depth of penetration of NIR
7 radiation is wavelength dependent, and varies with tissue type. Lammertyn et al. demonstrated that the depth of
8 penetration of NIR radiation varied from 2-3 mm at 900-1900 nm (5263 cm⁻¹-11111 cm⁻¹) to 4 mm at 700-900 nm (11111
9 cm⁻¹-14285 cm⁻¹) in an apple thickness study³². In another study, the depth of penetration in a neonatal head ranged from
10 6.3-8.5 mm in the 700-900 nm (11111 cm⁻¹-14285 cm⁻¹) spectral range³¹. Previous NIR studies with cartilage have
11 looked at the depth of penetration of NIR in cartilage^{25, 27}, with the primary goal being to ensure that the NIR radiation
12 penetrates through the sample thickness. However, studies of the depth of penetration of NIR radiation at different
13 wavelengths in cartilage are lacking. The average thickness of human cartilage is about 1-3 mm, and it changes according
14 to the location of cartilage^{33, 34} with age³⁵, and with disease, thinning as OA progresses. In order to ensure that the spectral
15 data collected is restricted to the tissue of interest i.e. cartilage in this case, and not from the underlying subchondral bone,
16 it is necessary to determine the depth of penetration of NIR in different wavelength regions. In the MIR, bone has a strong
17 phosphate absorbance at 900-1200 cm⁻¹³⁶ which can be used to differentiate the tissue from cartilage. However, in the
18 NIR spectral region of interest, there is no phosphate absorbance present. Therefore, the motivation of the current study
19 was to establish how the depth of penetration varies throughout the NIR frequency range (4000-10000 cm⁻¹) in cartilage.
20
21

22 **Material and methods**

23 **Material**

24 Cartilage plugs of 5 mm diameter (n=5) were harvested from freshly dissected newborn bovine knee joints (Research 87,
25 Boylston, MA). These plugs were cleaned to completely remove bone and were cut into varying thicknesses, ranging
26 from 0.5 mm to 5 mm using a tissue cutter (Zivic Instruments, Pittsburgh, PA). The thickness of each cartilage slice was
27 measured three times with a caliper (Fisher Scientific, Pittsburgh, PA) and averaged. Three to five replicates for each
28 tissue thickness were investigated.
29

30 **Near infrared fiber optic probe data collection**

31 NIR spectra were obtained using a 3 mm diameter silica glass NIR fiber optic reflectance probe (Art Photonics, Berlin,
32 Germany) coupled to a Matrix-F infrared spectrometer with a TE-InGaAs detector ((Bruker, MA). Background spectra
33 were collected from a mirrored surface. Sample spectra were collected from different thickness cartilage samples in
34 contact mode with and without a polystyrene plate underneath at 16 cm⁻¹ spectral resolution, with 256 co-added scans in
35 the 4000-10000 cm⁻¹ frequency range. A reference spectrum was collected from the polystyrene plate (thickness: 0.54
36 mm) to identify peaks of interest. A mirrored surface was placed underneath the polystyrene, and underneath the cartilage
37 samples when data was collected from cartilage alone. This results in a data collection mode of transreflectance for samples
38 1 mm or thinner. As the sample thickness increases, diffuse reflectance increasingly dominates the spectra.
39

40 **Near infrared imaging data collection**

41 NIR spectral imaging data were collected from 1 mm thick cartilage samples (n=3) to investigate the zonal distribution
42 of water and matrix components. The sections were cut longitudinally to obtain all the zones of the cartilage in one image.
43 To assess water distribution, cartilage sections were placed on glass slide, covered with a glass coverslip and sealed with
44 tape. NIR images were collected in transmission mode on a Perkin Elmer spotlight 400 spectrometer (Perkin Elmer,
45 Shelton, CT) at 32 cm⁻¹ spectral resolution, 16 co-added scans and at 50 μm spatial resolution in the 4000-7800 cm⁻¹
46 frequency range. For matrix distribution the samples were air dried and imaged using the same parameters. Transmittance
47 spectra were ratioed to a background obtained through the glass slide and converted to absorbance for data analysis. The
48 image acquisition time was approximately 15 minutes per sample.
49

50 **Data analysis**

51 NIR Spectra were processed using Unscrambler 10.1 (CAMO, Woodbridge, NJ). NIR spectra from cartilage with
52 different thicknesses were analyzed to understand the effect of an increase in thickness on the NIR spectrum. For the
53 data analysis the NIR spectral range was divided into 3 regions: 4000-5100 cm⁻¹, 5100-7000 cm⁻¹ and 7000-9000 cm⁻¹.
54 Polystyrene peaks were identified and assessed to determine the depth of penetration in each region separately. Spectra
55 from cartilage samples with and without polystyrene plate underneath were compared to determine the depth of
56 penetration of NIR. Spectra were first visually compared to see if the polystyrene peaks were visible in the raw cartilage
57 spectrum when the polystyrene plate was placed underneath during data collection. Further, second derivative spectra
58
59
60

1
2
3 were analyzed (Savitzky Golay, 31 point smoothing) to improve the assessment of the presence of polystyrene in the
4 cartilage spectra.
5

6 7 **Spectral Image analysis**

8 Images of integrated areas under the NIR water absorbances centered at 5200 and 6890 cm^{-1} were generated using ISYs
9 5.0 software (Malvern Instruments, UK) to assess the distribution of water in cartilage. Similarly, integrated images for
10 matrix distribution were generated from the 4384 cm^{-1} (combination of collagen and proteoglycan) absorbances²⁴.

11 **Results**

12 **Cartilage NIR spectra with varying thickness**

13 Cartilage NIR fiber optic spectra were dominated by water absorbances at 5200 cm^{-1} , 6890 cm^{-1} and 8500 cm^{-1} and matrix
14 peaks at $\sim 5600 \text{ cm}^{-1}$. Cartilage spectra with different thickness were compared to see the effect of increasing thickness on
15 the spectra (Figure 1). It was observed that as the thickness of the cartilage increased, the water absorbance band at 6890
16 and 8500 cm^{-1} broadened. We observed that not only did the peaks change as the thickness of the cartilage changed, the
17 mode of data acquisition also changed. When the thickness of the cartilage was less than 1 mm, the mode of data collection
18 was transreflectance, as the radiation could pass through the sample and reflect from the mirror back through the tissue.
19 However, as the thickness of the cartilage increased the mode of data collection was dominated by diffuse reflectance.
20

21 **Comparison of raw and second derivatives of the NIR spectra from cartilage of varying thickness with polystyrene 22 underneath**

23 The NIR spectrum of polystyrene (Figure 2) displays several distinct peaks (4048, 4245, 4330, 4612, 4663, 5668, 5949,
24 6078, 8270, and 8741 cm^{-1}) in the 4000-9000 cm^{-1} spectral region. The primary reason behind utilizing polystyrene in
25 this study was the fact that it had sharp peaks in the three regions of interest in the NIR spectrum. To assess the depth of
26 penetration of NIR in region 1, polystyrene absorbances at 4612 and 4663 cm^{-1} were assessed. Similarly, for regions 2
27 and 3, polystyrene absorbances at 5959 and 8741 cm^{-1} were assessed, respectively. The NIR spectrum of polystyrene,
28 cartilage of 0.5 mm thickness with polystyrene underneath and without polystyrene underneath are shown in Figure 3.
29 The polystyrene peaks are clearly visible in all three regions of the NIR spectra of cartilage with the polystyrene plate
30 underneath, which confirmed that the depth of penetration is at least 0.5 mm.
31

32
33 When raw spectra from a 1 mm thick cartilage specimen with and without polystyrene were compared (Figure 4), it was
34 observed that the polystyrene peaks in region 1 was no longer visible, but the polystyrene peaks in region 2 and region 3
35 were clearly observed. Second derivatives of the cartilage spectra with and without polystyrene were assessed to obtain
36 more accurate data on penetration. It was found that in the second derivative of 1 mm cartilage with polystyrene
37 underneath, polystyrene peaks were in fact still evident.
38

39 Similarly, we compared 2 mm thick cartilage spectra with and without polystyrene underneath (Figure 5). It can be seen
40 that the polystyrene peaks were not visible in region 1 but were still seen in regions 2 and 3, even though their intensity
41 was reduced compared to the 1 mm cartilage with polystyrene underneath. When second derivatives were evaluated, we
42 could barely see polystyrene in region 1, indicating the NIR penetration was reaching its limit.
43

44 In 3 mm thick cartilage with polystyrene underneath, polystyrene peaks were seen only in region 3 of the raw spectrum
45 (Figure 6). The evaluation of second derivative spectra showed that the polystyrene peak in region 1 was not seen at all,
46 whereas in region 2 it was approaching its penetration limit. However, the polystyrene peak in region 3 was clearly
47 observed.
48

49 The raw NIR spectra of 4 mm thick cartilage with and without polystyrene underneath looked very similar to each other
50 (Figure 7). The polystyrene peaks were not seen in any region of the spectrum obtained from cartilage with polystyrene
51 underneath. Evaluation of second derivative spectra showed that region 1 and region 2 had no polystyrene absorbances,
52 but region 3 clearly showed a polystyrene peak. We also observed that the second derivative NIR spectra of cartilage
53 with and without a polystyrene plate underneath were very similar in regions 1 and 2 as thickness increased, indicating
54 no polystyrene penetration.
55

56 **NIR image analysis results**

57
58
59
60

1
2
3 FTIR images of cartilage showed the distribution of water and matrix content across all the zones of cartilage (Figure 8).
4 The free water content (8B) was greatest just below the superficial zone, into the middle zone, and decreased towards the
5 deep zone. The bound plus free water (8A) showed a similar distribution, except for quite near the surface. The reduction
6 in water content towards the deep zone is consistent with literature reports². The matrix content similarly was greater near
7 the superficial zone, but decreased to a much greater extent into the middle and deeper zones.
8

9 Discussion

10 The current study showed that the depth of penetration of NIR radiation varies throughout the NIR spectral range in
11 cartilage from 0.5 mm to 5 mm. In region 1 (4000-5000 cm⁻¹), the NIR depth of penetration was at least ~1 mm, but
12 approached the penetration limit at 2 mm. In region 2 (5000-7000 cm⁻¹), the NIR depth of penetration was ~3 mm whereas
13 in region 3 (7000-9000 cm⁻¹) it was found to be greater than 4 mm.
14

15 Our results suggest that since the normal cartilage thickness of human cartilage is between 1-3 mm, the NIR
16 absorbances obtained from the tissue will arise from cartilage, as well as from the subchondral bone underneath it, if the
17 correct spectral range is not investigated. In NIR spectra, it is difficult to differentiate between bone and cartilage
18 absorbances as the NIR region investigated does not display a phosphate absorbance. NIR absorbances from bone and
19 cartilage, primarily water and organic matrix components, are at similar wavenumbers, though bone has sharper spectral
20 features³⁰. Therefore, the spectral region from 4000-7000 cm⁻¹, where the depth of penetration is ~3 mm, could be an
21 ideal region for cartilage assessment. However, the spectral contribution from the higher wavenumbers could be useful
22 for certain investigations focused on obtaining information from the subchondral bone.
23

24 A recent study from our group investigated the depth of penetration of bovine nasal cartilage (BNC) in the 4000-7000
25 cm⁻¹ spectral region³⁰. Here BNC samples were cut into different thickness from 0.34 to 5.76 mm and a parafilm
26 absorbance peak at 5774 cm⁻¹ was used to assess the depth of penetration. It was found the depth of penetration of NIR
27 radiation for BNC in the spectral range 5000-7000 cm⁻¹ was ~5 mm. In the current study where articular cartilage was
28 used, the depth of penetration was ~3 mm in the same spectral range. The main differences between BNC and articular
29 cartilage is the zonal organization in articular cartilage, and alignment of collagen fibrils. Thus, the difference between
30 NIR depths of penetration is likely attributable at least in part to these features. Another difference between that study
31 and the current study is the fact that our polystyrene plate was 0.54 mm thick whereas the parafilm was only ~ 0.1 mm
32 thick. This difference in plastic thickness would result in a change in overall pathlength the NIR radiation travels through
33 the samples and underlying plastic, resulting in what appears to be reduced penetration depth through the cartilage.
34 However, since the thickness of 0.54 mm is closer to what would be observed for subchondral bone, the results from the
35 current study more closely resemble the physiological condition. A previous study by Spahn et al. used a ratio of the NIR
36 water absorbance band at 7017 cm⁻¹ to the 8510 cm⁻¹ matrix absorbance, and considered this as an indicator of cartilage
37 water content²⁰. According to our results, the depth of penetration of NIR radiation at this spectral range is greater than 5
38 mm. Therefore the spectral absorbance collected in this region not only resulted from the cartilage but also from the
39 subchondral bone underneath.

40 The NIR spectral range we used in this study was from 4000-10000 cm⁻¹. The absorbances in this region arise from
41 combination, first and second overtones of the fundamental vibrations in the mid-infrared regions. The absorbance
42 intensity is inversely proportional to the order of overtone thus making the analysis difficult and complicated^{37, 38}. A
43 recent study from our group showed that the absorbances from cartilage matrix components, (collagen type II and
44 chondroitin sulfate), in the 4000-5000 cm⁻¹ spectral region, could be used to assess cartilage composition²⁴. Similarly, we
45 showed that the water absorbance at 5200 cm⁻¹, which arises from bound and free water, and the 6890 cm⁻¹ free water
46 absorbance, could be used to assess water content²³. Together, these studies show that the NIR spectral region from 4000-
47 7000 cm⁻¹ could prove to be an important region to assess cartilage quality based on matrix composition, and thus provide
48 support for focusing on this region for evaluation of tissue pathology.

49 Recently, NIR has been used to develop a non-destructive method to determine the thickness of cartilage²⁵. In that
50 study, NIR spectra were collected from 1.2 mm to 2.4 mm thick cartilage samples from bovine samples. Partial least
51 square (PLS) models with various NIR spectral ranges from 4000-12000 cm⁻¹ were built to correlate NIR spectra with
52 the cartilage thickness, with the results of the PLS varying from 53% to 93% for correct thickness prediction. The best
53 results were from the 5350-8850 cm⁻¹ region, and the lowest correlation from higher wavenumbers, i.e. 8000-12000 cm⁻¹.
54 According to our results, the depth of penetration of NIR radiation in this range is more than 4 mm. Therefore the
55 absorbance in this range are a combination of cartilage and the subchondral bone, and possibly primarily from subchondral
56 bone, which could result in a poor thickness prediction. However, it's also possible that the differences in subchondral
57 bone contributions in the spectra could aid in the thickness assessment in the lower frequency region.
58
59
60

1
2
3
4
5
6
7
8
9
10
11
12
13
14
15
16
17
18
19
20
21
22
23
24
25
26
27
28
29
30
31
32
33
34
35
36
37
38
39
40
41
42
43
44
45
46
47
48
49
50
51
52
53
54
55
56
57
58
59
60

There were some limitations of our study, including the fact that the tissue sections were cut parallel to the cartilage surface, and thus differences in organization or composition in different zones could impact the results. In essence, this means that samples of different thicknesses could contain either, e.g., both superficial and middle zone cartilage, or only middle or deep zone cartilage, or middle plus deep zone cartilage. Our results from the imaging data analysis showed that the distribution of water and matrix components varies among the different zones. This is most relevant to our fiber optic studies if thinner cartilage tissues are evaluated in the lower frequency NIR spectral regions, and there could be a question as to whether having the dense, collagenous superficial zone intact would result in reduced penetration depth. To address this, a separate experiment was conducted in a similar manner as the rest of the study with 1 mm samples that contained superficial and middle zone cartilage to assess whether the zonal differences did in fact affect the depth of penetration. We found that the NIR spectra collected from these samples on top of polystyrene showed polystyrene peaks in all regions, in agreement with the results presented previously (data not shown). Another issue to address is the fact that we did not evaluate degraded tissue samples. Degraded cartilage is less dense and fibrillated due to the loss of proteoglycans and damage to the collagen fibers. In this case, it is possible that the depth of penetration would be even greater through the tissue, compared to normal cartilage. Thus, it's possible that we should consider further limiting the spectral range of analysis for such samples if we want to exclude the contribution of subchondral bone. Human adult normal and degraded cartilage should be evaluated in future studies to confirm the depth of penetration of NIR radiation in these physiologically relevant tissues.

Potential applications of NIR probe evaluation of cartilage include for animal model studies, where a non-destructive method could be used to understand the effects of therapeutics and rehabilitation protocols in longitudinal studies. Clinically, intra-articular injuries are the most common injuries in young athletes, such as meniscus and ligament tears³⁹. Currently, arthroscopic evaluation is the gold standard method for investigation of symptoms related to early stages of cartilage degeneration. However, they can be somewhat subjective as they rely on the perception of the surgeon performing the procedure. The use of NIR probes has the potential to play an important role in monitoring early degeneration of cartilage for the high risk patients, such as those with prior anterior cruciate ligament or meniscus injury. Since the data obtained is less subjective than that from visual arthroscopy, it is possible that more precise results on how to stage cartilage could be obtained. Further, since arthroscopy is currently the preferred method for evaluation of intra-articular tissues, addition of NIR fiber optic probe data, which could be obtained through an arthroscopic port, could prove to be an important tool to study the pathology of injury and repair. Improved understanding of the features of the NIR spectra is critical for implementation of this methodology for tissue evaluation.

Conclusion

The results from this study demonstrated that the depth of penetration of NIR radiation into articular cartilage varies throughout the spectral range, 4000-10000 cm^{-1} , from 0.5 mm to at least 5 mm. The optimal NIR frequency range to ensure the absorbances being evaluated are only from cartilage and not from the subchondral bone is no higher than 7000 cm^{-1} .

Acknowledgements

This study was supported by NIH AR056145 and EB000744.

Reference

1. A. R. Poole, T. Kojima, T. Yasuda, F. Mwale, M. Kobayashi and S. Laverty, *Clinical orthopaedics and related research*, 2001, S26-S33.
2. M. Huber, S. Trattnig and F. Lintner, *Investigative Radiology*, 2000, 35, 573-580.
3. T. Neogi and Y. Zhang, *Rheumatic Disease Clinics of North America*, 2013, 39, 1-19.
4. M. Huber, S. Trattnig and F. Lintner, *Invest Radiol*, 2000, 35, 573-580.
5. A. I. Caplan, M. Elyaderani, Y. Mochizuki, S. Wakitani and V. M. Goldberg, *Clinical orthopaedics and related research*, 1997, 254-269.
6. S. Oakley, I. Portek, Z. Szomor, R. Appleyard, P. Ghosh, B. Kirkham, G. Murrell and M. Lassere, *Osteoarthritis and cartilage*, 2005, 13, 368-378.
7. N. Maffulli, U. G. Longo, S. Campi and V. Denaro, *Evidence-Based Orthopedics*, 2012, 803-811.
8. R. Crawford, G. Walley, S. Bridgman and N. Maffulli, *British medical bulletin*, 2007, 84, 5-23.
9. G. Spahn, H. M. Klinger, M. Baums, U. Pinkepank and G. O. Hofmann, *Archives of orthopaedic and trauma surgery*, 2011, 131, 377-381.
10. G. Spahn, H. M. Klinger and G. O. Hofmann, *Archives of orthopaedic and trauma surgery*, 2009, 129, 1117-1121.
11. A. Billaud, A. Moreau-Gaudry, D. Girardeau-Montaut, F. Billet, D. Saragaglia and P. Cinquin, *J Bone Joint Surg Proc*, 2013, 95, 26-26.
12. M. F. Koff, K. K. Amrami and K. R. Kaufman, *Osteoarthritis Cartilage*, 2007, 15, 198-204.

13. S. Lusse, H. Claassen, T. Gehrke, J. Hassenpflug, M. Schunke, M. Heller and C. C. Gluer, *Magn Reson Imaging*, 2000, 18, 423-430.
14. W. Marik, S. Apprich, G. Welsch, T. Mamisch and S. Trattinig, *European Journal of Radiology*, 2012, 81, 923-927.
15. Ding C, F. C and a. G. J, *Nat Clin Pract Rheumatol*, 2008, 4, 4-5.
16. M. P. Recht, D. W. Goodwin, C. S. Winalski and L. M. White, *AJR. American journal of roentgenology*, 2005, 185, 899-914.
17. I. Notingher and R. E. Imhof, *Skin Research and Technology*, 2004, 10, 113-121.
18. S. Wartewig and R. H. Neubert, *Advanced drug delivery reviews*, 2005, 57, 1144-1170.
19. I. O. Afara and A. Oloyede, *Near Infrared Spectroscopy Evaluation of Articular Cartilage: Decision-Making in Arthroplasty: Real-Time Assessment of Articular Cartilage*, LAP Lambert Academic Publishing 2012.
20. G. Spahn, H. Plettenberg, E. Kahl, H. M. Klinger, T. Muckley and G. O. Hofmann, *BMC Musculoskelet Disord*, 2007, 8, 47.
21. G. Spahn, H. Plettenberg, H. Nagel, E. Kahl, H. M. Klinger, T. Muckley, M. Gunther, G. O. Hofmann and J. A. Mollenhauer, *Med Eng Phys*, 2008, 30, 285-292.
22. D. Baykal, O. Irrechukwu, P. C. Lin, K. Fritton, R. G. Spencer and N. Pleshko, *Applied spectroscopy*, 2010, 64, 1160-1166.
23. M. V. Padalkar, R. G. Spencer and N. Pleshko, *Ann Biomed Eng*, 2013, 41, 1-11.
24. U. P. Palukuru, C. M. McGoverin and N. Pleshko, *Matrix Biology*, 2014.
25. I. Afara, S. Singh and A. Oloyede, *Med Eng Phys*, 2012, 35, 88-95.
26. I. Afara, S. Singh and A. Oloyede, *J Mech Behav Biomed*, 2012, 249-258.
27. C. P. Brown, J. C. Bowden, L. Rintoul, R. Meder, A. Oloyede and R. W. Crawford, *Phys Med Biol*, 2009, 54, 5579-5594.
28. G. Spahn, G. Felmet and G. O. Hofmann, *Arch Orthop Trauma Surg*, 2013, 133, 1-6.
29. I. Afara, I. Prasadam, R. Crawford, Y. Xiao and A. Oloyede, *Osteoarthr Cartil*, 2012, 20, 1367-1373.
30. McGoverin CM, Lewis K, Yang X, Bostrom MPG and P. N, *Applied spectroscopy*, 2014, 68, 1168.
31. F. Faris, M. Thorniley, Y. Wickramasinghe, R. Houston, P. Rolfe, N. Livera and A. Spencer, *Clin Phys Physiol Meas*, 1991, 12, 353.
32. J. Lammertyn, A. Peirs, J. De Baerdemaeker and B. Nicolai, *Postharvest Biol Technol*, 2000, 18, 121-132.
33. G. Li, S. E. Park, L. E. DeFrate, M. E. Schutzer, L. Ji, T. J. Gill and H. E. Rubash, *Clinical biomechanics*, 2005, 20, 736-744.
34. D. Shepherd and B. Seedhom, *Annals of the rheumatic diseases*, 1999, 58, 27-34.
35. R. Karvonen, W. Negendank, R. Teitge, A. Reed, P. Miller and F. Fernandez-Madrid, *The Journal of rheumatology*, 1994, 21, 1310-1318.
36. A. Boskey and N. Pleshko Camacho, *Biomaterials*, 2007, 28, 2465-2478.
37. H. Büning-Pfaue, *Food Chemistry*, 2003, 82, 107-115.
38. H. Cen and Y. He, *Trends in Food Science & Technology*, 2007, 18, 72-83.
39. D. M. Swenson, C. L. Collins, T. M. Best, D. C. Flanigan, S. K. Fields and R. Comstock, 2005.

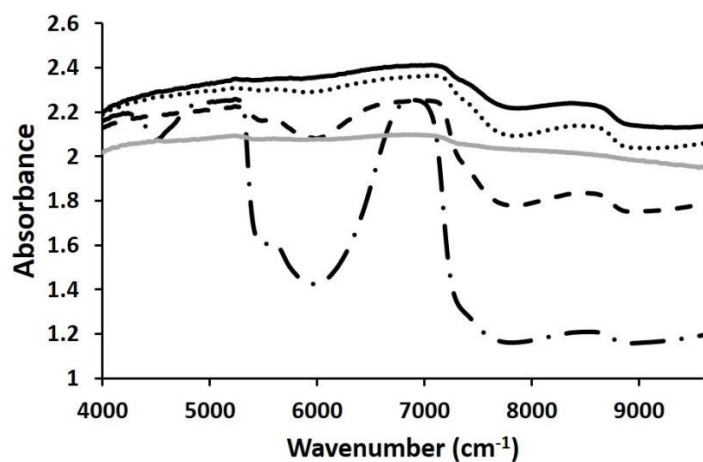


Figure 1: NIR cartilage spectra from 1 mm (long dash dot), 2 mm (black dash), 3 mm (dots) and 4 mm (solid black) thick samples. A diffuse reflectance spectrum (solid grey) obtained from a 1 mm thick cartilage sample on a dark surface is added for comparison of transfectance (long dash dot) to diffuse reflectance in the thin sample.

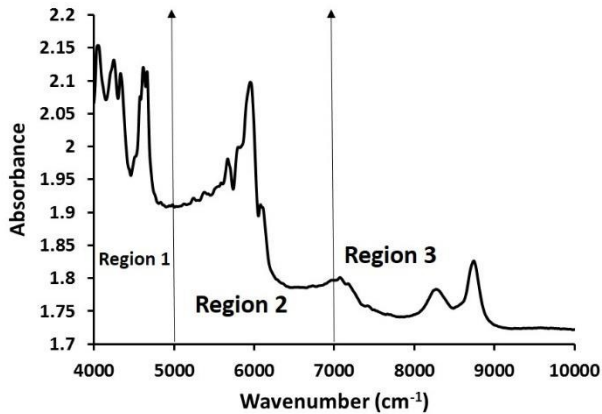


Figure 2: NIR spectrum of polystyrene. The NIR spectra were divided into 3 regions; region 1 (4000-5000 cm⁻¹), region 2 (5000-7000 cm⁻¹) and region 3 (7000-9000 cm⁻¹).

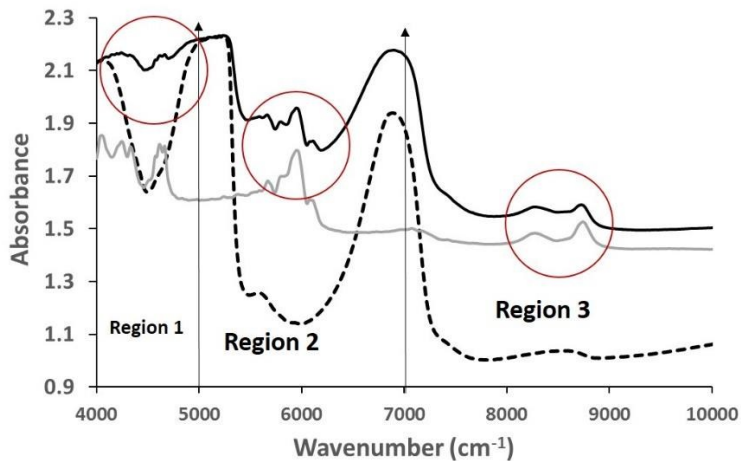


Figure 3: Comparison of raw NIR spectra from 0.5 mm thick cartilage sample with polystyrene (solid black) and without polystyrene underneath (dotted black) along with polystyrene spectrum (solid grey). The influence of the polystyrene peak is highlighted with red circles in the three regions.

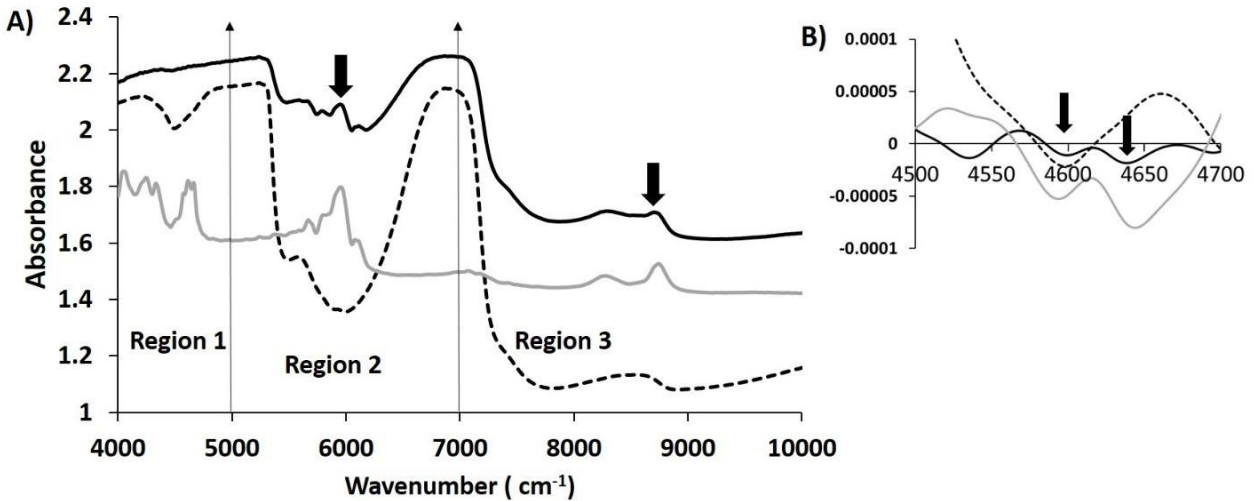


Figure 4: A) Comparison of raw NIR spectra from 1 mm thick cartilage with polystyrene (solid black) and without polystyrene (dotted black) along with polystyrene spectra (solid grey). Influence of polystyrene on NIR spectra of 1 mm cartilage in region 2 and region 3 is highlighted by arrows. B) Second derivatives of NIR spectra from 1 mm thick cartilage with polystyrene underneath (solid black) and without polystyrene (dotted black) along with polystyrene spectra (solid grey) are compared in region 1. The polystyrene spectrum was divided by a factor of 10 to bring all spectra on the same scale.

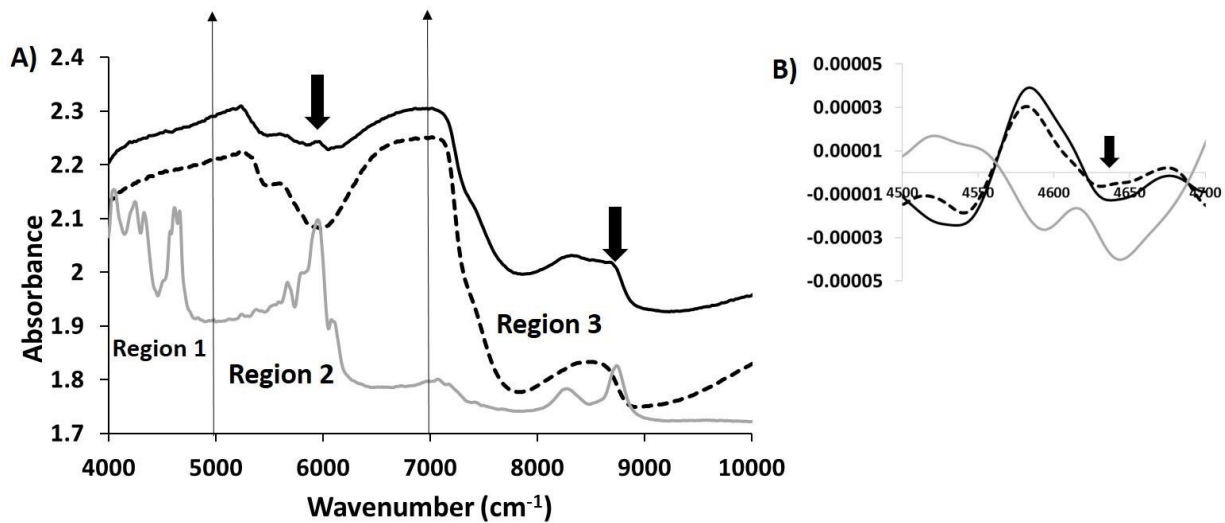


Figure 5: A) Comparison of raw NIR spectra from 2 mm thick cartilage with polystyrene (solid black) and without polystyrene (dotted black) along with polystyrene spectra (solid grey). Influence of polystyrene on NIR spectra of 2 mm cartilage in region 2 and region 3 is highlighted by arrows. B) Second derivatives of NIR spectra from 2 mm thick cartilage with polystyrene underneath (solid black) and without polystyrene (dotted black) along with polystyrene spectra (solid grey) compared in region 1. The polystyrene spectrum was divided by a factor of 10 to bring all spectra on the same scale.

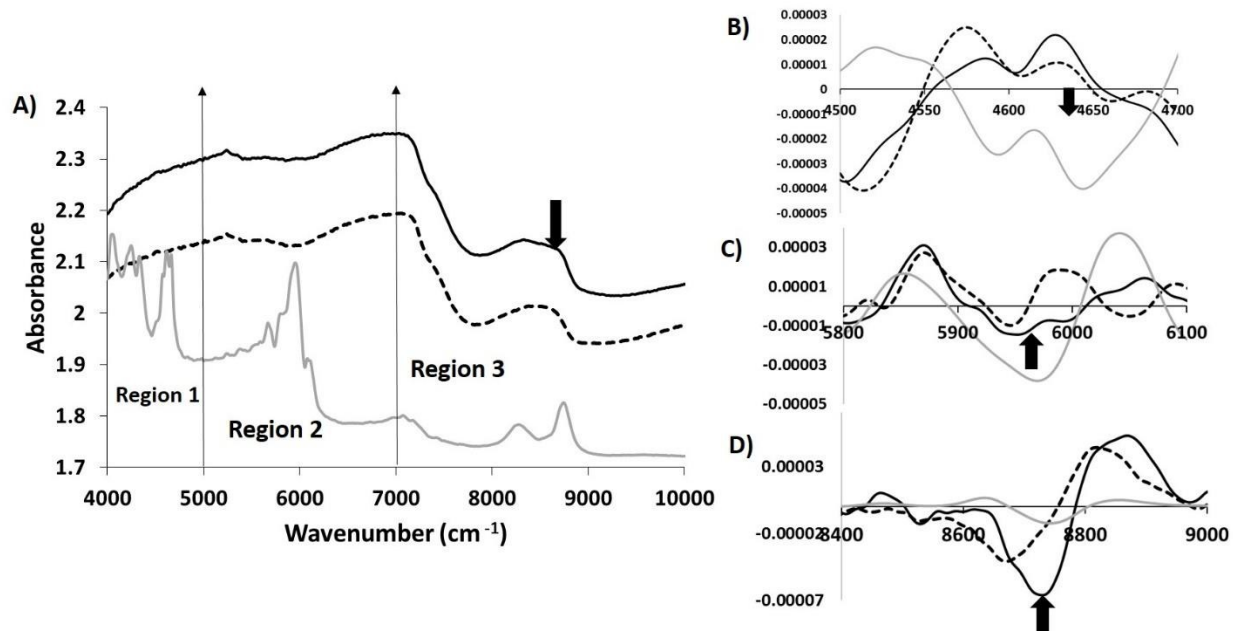


Figure 6: A) Comparison of raw NIR spectra from 3 mm thick cartilage with polystyrene (solid black) and without polystyrene (dotted black) along with polystyrene spectra (solid grey). Second derivatives of NIR spectra from 3 mm thick cartilage with polystyrene (solid black) and without polystyrene (dotted black) along with polystyrene spectra (solid grey) compared in region 1 (B), region 2(C) and region 3(D). The polystyrene spectrum was divided by a factor of 10 to bring all spectra on the same scale.

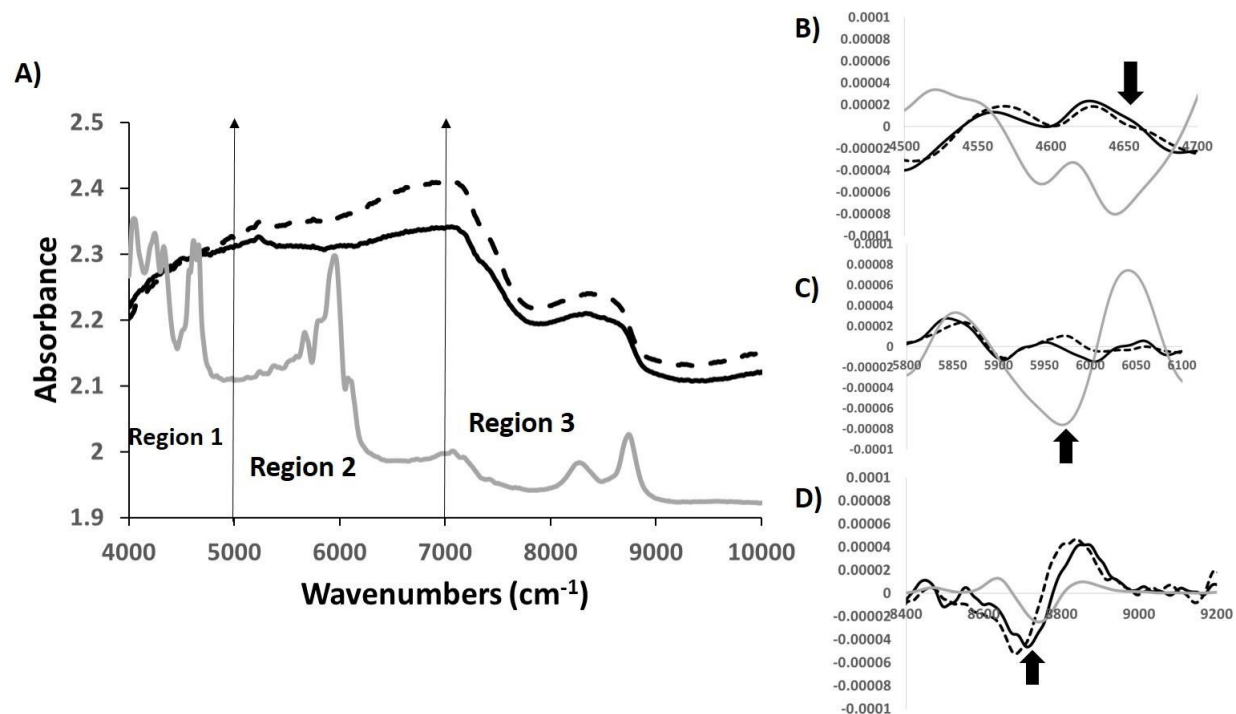


Figure 7: A) Comparison of raw NIR spectra from 4 mm thick cartilage with polystyrene (solid black) and without polystyrene (dotted black) along with polystyrene spectra (solid grey). Second derivatives of NIR spectra from 4 mm thick cartilage with polystyrene (solid black) and without polystyrene (dotted black) along with polystyrene spectra (solid grey) compared in region 1 (B), region 2(C) and region 3(D). The polystyrene spectrum was divided by a factor of 10 to bring all spectra on the same scale.

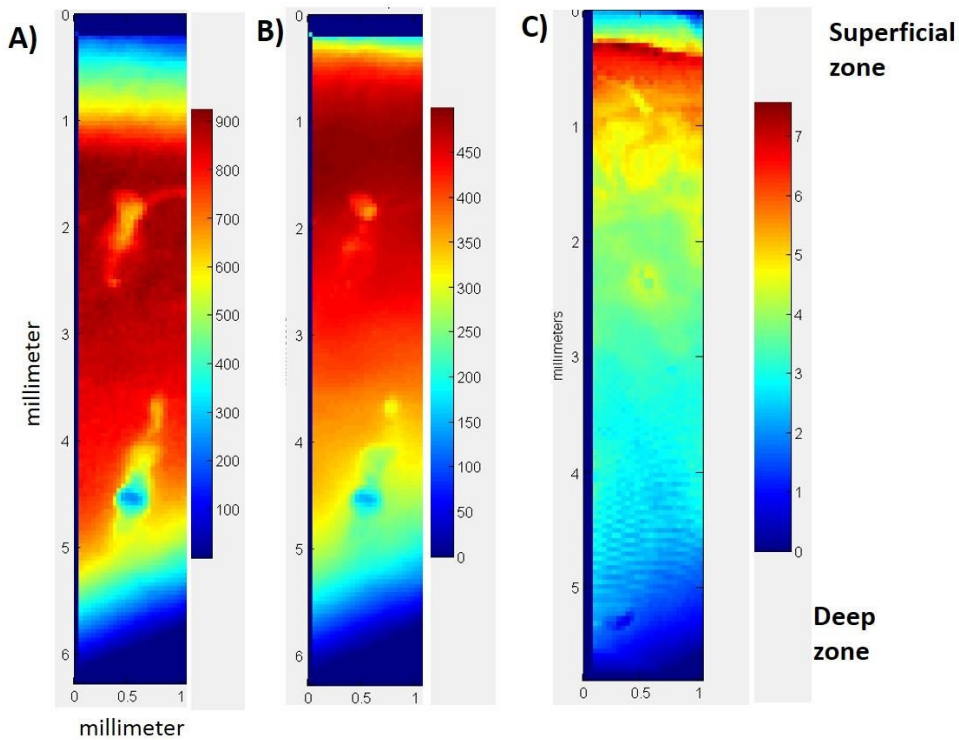


Figure 8: Distribution of water (A and B) and matrix components (C) through the cartilage depth. A) Integrated area map of the 5200 cm^{-1} (bound and free water) NIR absorbance B) Integrated area map of the 6800 cm^{-1} (free water) NIR absorbance and C) Integrated area map of the 4384 cm^{-1} (combination of collagen and proteoglycan) NIR absorbance. Color bar shows the integrated area scale for each absorbance.